Neuromethods 2780

Springer Protocols

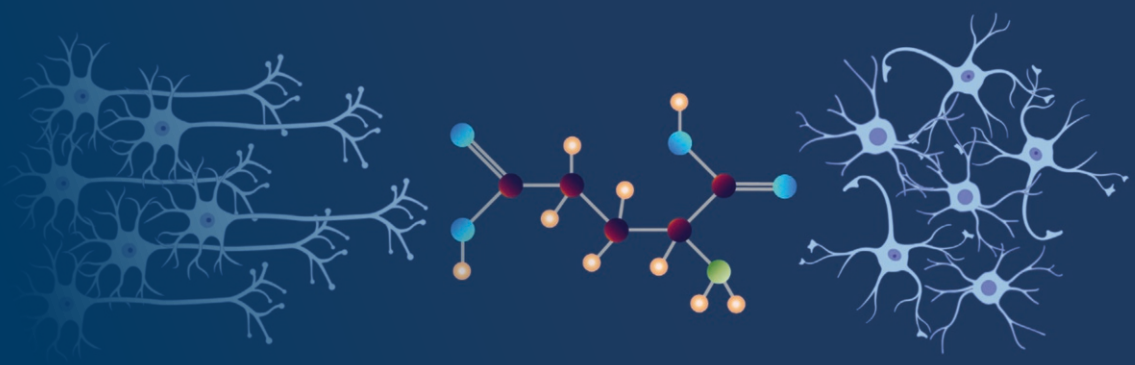

Maria Kukley *Editor*

New Technologies for Glutamate Interaction

Neurons and Glia

MOREMEDIA

Humana Press

Chapter 1

Visualization of Glutamatergic Neurotransmission in Diverse Model Organisms with Genetically Encoded Indicators

Abhi Aggarwal, Joyce Chan, Amelia K. Waring, Adrian Negrean, Jonathan S. Marvin, Kaspar Podgorski, and Loren L. Looger

Abstract

Glutamate is the principal excitatory neurotransmitter, and occasionally subserves inhibitory roles, in the vertebrate nervous system. Glutamatergic synapses are dense in the vertebrate brain, at ~$1/\mu m^3$. Glutamate is released from and onto diverse components of the nervous system, including neurons, glia, and other cells. Methods for glutamate detection are critically important for understanding the function of synapses and neural circuits in normal physiology, development, and disease. Here we describe the development, optimization, and deployment of genetically encoded fluorescent glutamate indicators. We review the theoretical considerations governing glutamate sensor properties from first principles of synapse biology, microscopy, and protein structure-function relationships. We provide case studies of the state-of-the-art iGluSnFR glutamate sensor, encompassing design and optimization, mechanism of action, in vivo imaging, data analysis, and future directions. We include detailed protocols for iGluSnFR imaging in common preparations (bacteria, cell culture, and brain slices) and model organisms (worm, fly, fish, rodent).

Key words Glutamate, iGluSnFR, Biosensors, Imaging, Synapses

1 Introduction

Glutamate is the predominant excitatory neurotransmitter in vertebrates and many invertebrates and subserves inhibitory roles in both clades. It functions in both the central and peripheral nervous systems and in diverse organ systems. Glutamatergic synapses form the bulk of contacts in the brain. Glutamate interacts with AMPA, NMDA, and kainate ionotropic receptors as well as diverse metabotropic receptors, with each receptor type serving distinct roles in neural signalling. More is known about glutamatergic signaling

Abhi Aggarwal and Joyce Chan contributed equally.

Maria Kukley (ed.), *New Technologies for Glutamate Interaction: Neurons and Glia*, Neuromethods, vol. 2780,
https://doi.org/10.1007/978-1-0716-3742-5_1,

than any other transmitter; however, a great number of aspects remain mysterious. In this chapter, we review recent advances in directly visualizing glutamatergic neurotransmission using engineered genetically encoded biosensors alongside advances in (sub)cellular-resolution imaging. We focus on key aspects of glutamatergic signaling that are best revealed through optical imaging and in particular on detailed methods for state-of-the-art glutamate imaging in a range of common model organisms and preparations. We also point the reader to technical discussions of various aspects of glutamate imaging.

2 Discovery of Glutamate as a Neurotransmitter

The detection of glutamatergic neurotransmission has had a long history. Even the identification of glutamate as a neurotransmitter was itself a multi-decade process. Glutamate is abundant in all cells, as it is a common amino acid in proteins and a central player in multiple metabolic pathways including glycolysis, the TCA cycle, and pyrimidine metabolism. That the concentration of glutamate in the brain (~5–10 mM) is several times higher than any other amino acid, despite other amino acids being more abundant in proteins, is insufficient evidence that glutamate plays a role as a signaling molecule. Injection of glutamate into the brains of dogs produced convulsions [1], hinting that the molecule could signal, but these experiments did not confirm any physiological role. About this time, though, the development of electrophysiological methods such as patch-clamping and current amplification allowed direct testing of the effects of compounds such as glutamate on diverse preparations. Jeffery Watkins set about in early 1958 to identify hitherto unknown neurotransmitters using this approach [2, 3]. Importantly, GABA had already been identified as an inhibitory neurotransmitter and was used as a control. Watkins et al. injected electrical current into the dorsal roots of isolated spinal cords of cane toads and recorded from downstream ventral root neurons [4]. Bath application of compounds activated various receptors, modulating the baseline response (clear depolarization). GABA decreased the peak of the evoked signal, consistent with its inhibitory role. Intriguingly, application of low millimolar glutamate increased the response, but higher concentrations (>10 mM) decreased it again [4]. This further cemented the notion of glutamate as a transmitter molecule, but direct interpretation was confounded by the opposing activities of glutamate at different points in the spinal cord circuit.

Other agonists were soon discovered. Notably, the excitatory effect of aspartate was similar to that of glutamate, and (confusingly) both the D- and L-enantiomers of both amino acids were active. The excitatory effect of these chemicals was confounded by

the fact that Renshaw interneurons, which mediate the contraction and relaxation of complementary muscles, were also activated by glutamate, giving rise to the idea that glutamate might be "non-specific." Throw in the fact that homocysteine and N-methyl-D-aspartate (NMDA) appeared to be even more potent than glutamate or aspartate, and the specificity of glutamate as a neurotransmitter remained an unresolved question until 1977. In a crucial experiment with individual Renshaw cells, with excitation by microelectrophoretic administration of glutamate or acetylcholine, stimulation of dorsal or ventral roots, and application of the cholinergic antagonist dihydroxydibutylether (DHbE) or the glutamatergic antagonist D-α-aminoadipate, it was shown that L-glutamate was responsible for excitation of Renshaw cells from incoming dorsal root cells [5].

Soon the various receptors of glutamate were discovered and cloned, showing that fast synaptic responses arose from ionotropic glutamate channels/receptors (iGluRs) and slower signals arose from metabotropic, G-protein-coupled glutamate receptors (mGluRs). This discovery led to the use of patch-clamping to measure excitatory postsynaptic currents (EPSCs) arising from inputs to glutamatergic synapses. However, such recordings are technically challenging and very invasive, are limited to single cells at a time, and integrate the inputs into all synapses, reflecting only bulk activity. Investigation of the activities of single glutamatergic synapses would require the development of other techniques.

3 Key Aspects of Glutamatergic Signaling

Glutamatergic synapses are ubiquitous in the brain. In the vertebrate brain, most glutamatergic synapses are characterized by the presence of an obvious presynaptic terminal and a small protrusion from a postsynaptic dendrite known as a spine. Spines typically vary between ~0.1 and 2 microns (some are larger) and can vary in length, diameter, and shape across brain regions, cell types, and synaptic strength. Spines consist of a bulbous head containing key postsynaptic proteins such as glutamate receptors and a narrow neck connecting the spine to the dendritic shaft (Fig. 1a). Glutamate is released from the presynaptic terminal through exocytosis of synaptic vesicles, each containing ~500 molecules. Every step of glutamate transmission is quite rapid, with the whole process typically lasting <10 milliseconds [6] (Fig. 1b). Exocytosis occurs within microseconds of terminal depolarization, with glutamate levels in the synaptic cleft (20–30 nm; zeptoliter-scale) peaking within a millisecond. Glutamate is cleared from the synaptic cleft just as rapidly, as fast, high-affinity transporters located on neurons and closely apposed astrocytes clear glutamate within another few milliseconds, preventing excitotoxicity from excessive stimulation

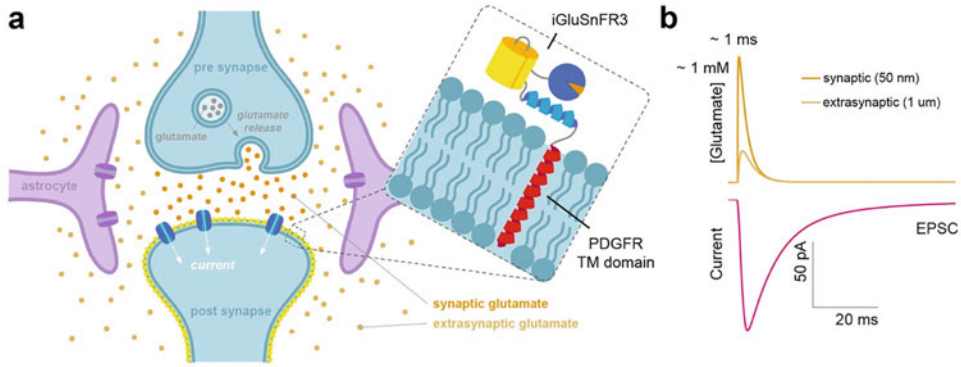

Fig. 1 Glutamatergic synapses and glutamate transients. (**a**) Left, schematic of glutamatergic synapse, showing a presynaptic terminal with a docked glutamatergic vesicle, a postsynaptic spine head with glutamate receptors, and glutamate transporters expressed on closely apposed astrocytes. Right, cartoon of the iGluSnFR3 glutamate sensor expressed in the spine head membrane with PDGFR transmembrane domain shown in red. (**b**) Approximate waveforms of glutamate concentrations (synaptic and extrasynaptic) and resulting excitatory postsynaptic current, in response to single-vesicle release. Waveforms are derived from models incorporating the field's understanding of glutamate dynamics. More details can be found in [23]

and critically largely limiting the spatial extent of glutamate signaling to direct postsynaptic contacts. Despite rapid clearance, glutamate can in some circumstances escape the synaptic cleft and enter the extracellular milieu, where it can access and activate other nearby (<~1–2 microns) spines and receptors located along the dendritic shaft [7], in a process known as "spillover."

Neurons routinely have highly branched dendritic arbors, with thousands of spines on each branch. Glutamatergic inputs into individual spines summate over local extent and can lead to the firing of dendritic Ca^{2+} spikes, further enhancing the degree of neuronal activation [8]. Cation flux through ionotropic glutamate receptors is sufficient to produce detectable electrical depolarization at the cell body, even if quite distant.

Major questions regarding glutamatergic signaling remain insufficiently answered, including (but definitely not limited to):

- What is the nature of the transformation from glutamate molecules to receptor activation to spine depolarization?
- What is the spatial extent of glutamate spread from single release sites under diverse activity conditions?
- What is the transformation from activation of single and nearby spines to dendritic spikes?
- What is the transformation from spine inputs and dendritic spikes to subthreshold depolarization at the cell body and action potential initiation, at the level of glutamate, Ca^{2+}, other secondary messengers, and membrane potential?

- What is the nature of the distribution of spines along dendritic segments in terms of activity tuning?
- How quickly can the activity tuning profiles of single spines change?
- How are glutamate transporters regulated by neural and glial activity, by brain state, and by disease?
- Is glutamate ever released from astrocytes and other glia, and under what circumstances?
- What is the role of microglial glutamate transporters in health and disease?

Addressing these questions and many more issues at the core of cellular and circuit neuroscience requires methods for the *direct* detection of glutamate, rather than inferring its presence from indirect readouts, such as electrical depolarization, Ca^{2+} ions, etc. We cover such methods in the next section, leading up to the development of the state-of-the-art genetically encoded glutamate indicators discussed in the remainder of the chapter.

4 Glutamate Detection Methods

Measurement of glutamatergic signaling at multiple cells and at single synapses requires a mechanism to transduce glutamate into a macroscopic observable—ideally one suited to high spatial and temporal resolution imaging. Early experiments used glutamate oxidase-linked reporters [9], but signal and resolution were quite poor, and readout was indirect. With the cloning and characterization of glutamate-specific, micromolar-affinity bacterial periplasmic binding proteins [10], the door was opened to engineering of high-quality molecular sensors. The uncharacterized protein YbeJ (later renamed GltI) was cloned, expressed, and found to bind glutamate. Incorporation of single cysteine residues and coupling of environmentally sensitive small-molecule fluorophores yielded robust hybrid protein small-molecule glutamate sensors [10]. Fusion of cyan and yellow fluorescent proteins led to the first fully genetically encoded fluorescent sensor, FLIPE [11] (Fig. 2a). The signal change was low, with a CFP:YFP fluorescence resonance energy transfer (FRET) ratio change of 8% in response to K^+-induced depolarization of cultured neurons. Several years later, a similar sensor, concurrently developed as glutamate-sensing fluorescent reporter (GluSnFR) [12], was optimized by mutation of the linkers connecting the CFP and YFP to the N- and C-termini of the binding protein. The improved "SuperGluSnFR" was able to detect electrically stimulated glutamate release in neuronal culture [13]. Signal was improved over FLIPE but still insufficient for in vivo use.

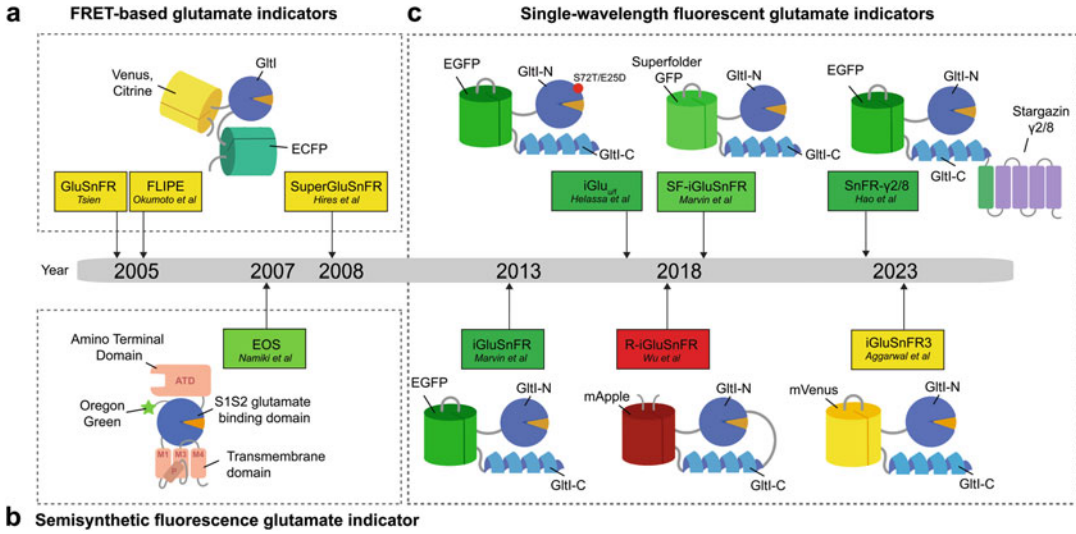

Fig. 2 Development of genetically encoded fluorescent indicators for glutamate. (**a**) Schematic of fluorescence resonance energy transfer (FRET)-based glutamate sensors, such as GluSnFR, FLIPE, and SuperGluSnFR. (**b**) Schematic of the semisynthetic fluorescent indicator glutamate optical sensor (EOS). Here, the small-molecule dye Oregon Green produces indicator fluorescence in a fashion modulated by glutamate binding to the iGluR component. (**c**) Single-wavelength fluorescent glutamate indicators, such as iGluSnFR, $iGlu_u$, R^{ncp}-iGluSnFR, SF-iGluSnFR, SnFR-γ2, and iGluSnFR3. Unless otherwise shown, the soluble forms of indicators are fused to an N-terminal secretion peptide and a C-terminal fusion to traffic and anchor the sensor to the outside of the cell membrane in mammalian cells

Replacement of the CFP-YFP FRET pair with a single circularly permuted green fluorescent protein (cpGFP), inspired by the signaling mechanism of the GCaMP family of calcium indicators [14, 15], produced iGluSnFR ("i" for intensiometric), where glutamate binding led to an almost fivefold increase in fluorescence emission intensity [16]. In awake, behaving mice, iGluSnFR showed ~30% fluorescence increases to single bursts of glutamatergic signaling. Notably, iGluSnFR has been used for several important biological discoveries, such as the classification of bipolar cells in the mouse retina [17]. However, signal change of this first sensor version is insufficient for many applications, particularly in deep scattering tissue.

Thus, a second generation of iGluSnFR variants was developed [18] by (a) incorporation of the superfolder GFP mutations [19] to improve protein stability and expression level (this generation was thus dubbed "SF-iGluSnFR"), (b) modulating affinity through rational design, and (c) tuning of indicator color through chromophore mutagenesis. Affinity was increased or decreased, respectively, by mutations altering the open-closed equilibrium, specifically by decreasing or increasing the binding off-rate. SF-iGluSnFR was substantially brighter and more photostable in multiple in vivo preparations and supported long, high-signal-to-noise-ratio (SNR) imaging sessions, even under intense illumination

almost a millimeter below the pia [20]. The faster off-rate SF-iGluSnFR variant also facilitated better resolution of individual events in trains of glutamate signals.

The stabilization of the SF-iGluSnFR scaffold also facilitated the development of variants in different color channels through chromophore mutagenesis. Introducing targeted mutations, followed by reoptimization of linker regions, produced an excellent yellow variant, SF-Venus-iGluSnFR, and modestly performing cyan and blue variants. In addition to permitting two-color functional imaging, the yellow variant is compatible with high-speed (kilohertz frame-rate) two-photon imaging using various high-speed imaging methods like Scanned Line Angular Projection (SLAP) [21] microscopy, which make use of powerful 1030 nm laser lines.

Despite these improvements, SF-iGluSnFR has SNR too low for many imaging preparations, its kinetics are substantially slower than those of glutamate transients themselves, and given its pan-membrane localization, it reports all sources of glutamate, including extrasynaptic glutamate. In the next section, we discuss the diverse tunable properties of biosensors and the best combinations of parameters for addressing specific biological questions.

5 What Are the Properties of an Ideal Glutamate Sensor?

Glutamate sensors must, first and foremost, have the properties expected of any sensor used for in vivo imaging: good brightness, high photostability, excellent signal change upon ligand binding, minimal interference with cellular functions, and proper folding, fluorophore maturation, and targeting.

Ideal glutamate-binding affinity will depend on application: higher affinity will yield greater signal change for small events but runs the risk of quickly becoming saturated. Furthermore, a high-affinity sensor will be more sensitive to small amounts of glutamate entering from nearby but not directly connected synapses, i.e., spillover. Glutamate spillover is of course functionally relevant to neural computations [7], as glutamate receptors on the spine head, and particularly on the spine neck, respond with cation influx whatever the source of the glutamate molecules. For studies focused on determining spine-tuning properties, however, such detection of spilled-over glutamate confounds interpretation. As such, indicators that are not easily saturated are preferred for recorded individual synapses, as they will respond proportionately to the large amounts of glutamate arriving from synaptically connected neurons versus the small amounts from spillover.

Sensor kinetics (both rise and decay) are critically important for glutamate imaging and depend on the preparation and target application. Fast indicator kinetics—particularly risetime—are, of course, required to accurately reflect the few milliseconds timescales

of glutamate release events. The most important measure of kinetics is the rate of rise of indicator fluorescence (i.e., on-rate). Fast on-rates generate larger responses and allow the timing of events to be precisely determined. Due to the multi-step kinetics of fluorescent indicators (i.e., rapid binding followed by slower transition to brightly fluorescent state), on-rate depends on glutamate concentration and may saturate during brief, high-concentration synaptic release events. Rapid decay kinetics (off-rate) can be desirable to avoid saturation, but increasing off-rates result in smaller-amplitude, briefer signals that can be difficult to detect in challenging imaging conditions because of the small numbers of detected photons involved. Instrumentation is an important factor; fast imaging rates are necessary to take advantage of rapid indicators.

Indicator targeting determines many aspects of imaging experiments. Indicators expressed across the cellular membrane will report glutamate arising from all sources, and more importantly almost all sensor molecules will not be exposed to glutamate at all and as such constitute a large reservoir of unchanging background fluorescence, degrading SNR. Ideally, sensors should be localized to the expected sites of glutamate release and/or reception. It should be noted, however, that (1) photostability of membrane-localized indicators can be limiting, as they only diffuse in two dimensions, and (2) tethering probes to fixed locations can further limit diffusion and photostability. Lastly, fusing sensors to synaptic proteins runs the risk of disrupting the function of both the sensor and its fusion partner. Thus, sensors localized specifically and solely to small locales such as the presynaptic terminal and/or spine head should be tested carefully for brightness, photostability, and potential effects on synaptic function.

Overall, fast rise/decay kinetics and access of sensors to the center of the spine head are the properties that have been least well developed in existing glutamate sensors (whereas brightness, photostability, and signal change have been much more improved). Also, the affinity of existing glutamate indicators has been sufficiently high that they should be considered to report both synaptic and spilled-over glutamate.

6 iGluSnFR3

Having created the initial iGluSnFR scaffold and optimized it to the second-generation SF-iGluSnFR sensors, we recently set about to bring the performance of the sensor closer to that of an ideal glutamate sensor (Fig. 3a), as discussed in the previous section.

Foremost, we sought to improve the signal-to-noise ratio (SNR) of iGluSnFR through targeted mutagenesis, primarily by lowering the fluorescence of the glutamate-free sensor while maintaining that of the glutamate-bound sensor (Fig. 3b–e). High SNR

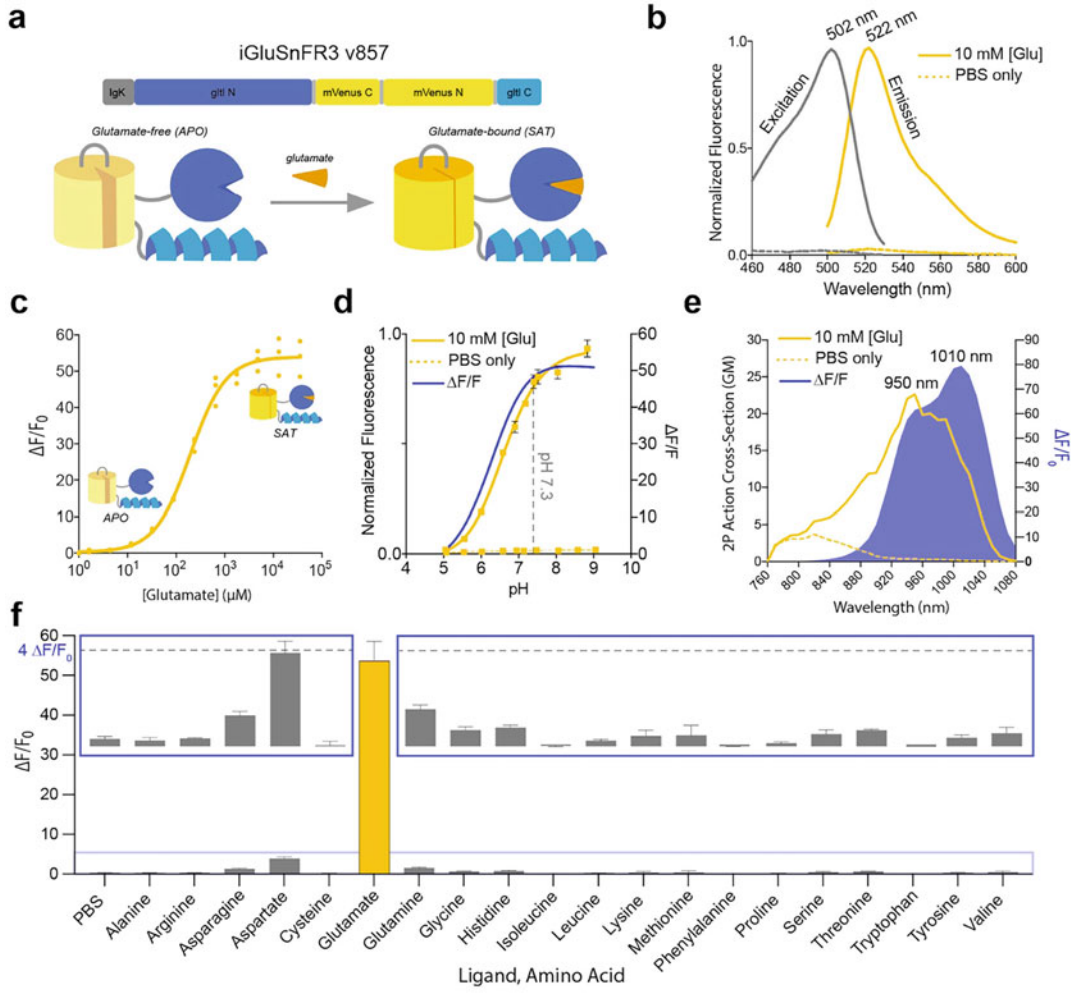

Fig. 3 Design and photophysical properties of the genetically encoded glutamate indicator iGluSnFR3. (**a**) Top, linear DNA schematic and bottom, protein schematic of iGluSnFR3 variant v857 consisting of a circularly permuted fluorescent protein inserted into the glutamate-binding protein gltI. (**b**) One-photon excitation and emission spectra of iGluSnFR3 in the presence and absence of glutamate. (**c**) Glutamate titration of iGluSnFR3 in purified protein. (**d**) pH titration and $\Delta F/F_0$ of iGluSnFR3 in purified protein. Typical physiological pH shown. (**e**) Two-photon excitation spectra and $\Delta F/F_0$ of iGluSnFR3. (**f**) $\Delta F/F_0$ of iGluSnFR3 in purified protein for additions of the 20 canonical L-amino acids. Top: zoom of all responses other than L-glutamate

facilitates imaging in multiple ways: (1) it improves the quality of all imaging; (2) it permits users to lower excitation power, improving photostability and decreasing photodamage; (3) it allows users to image larger fields of view and/or at faster rates; and (4) it permits users to sacrifice signal by, for instance, localizing the sensor to small volumes of interest. Dramatically lowering the glutamate-free fluorescence by reducing absorption also directly increases photostability, as the sensor is only bleachable when the chromophore is bright. The second primary focus of iGluSnFR3 engineering was

increasing the effective on-rate of the sensor, i.e., the speed at which fluorescence develops following exposure to glutamate. The design cycle yielded two iGluSnFR variants with excellent performance along these two metrics [22]: iGluSnFR3.v82 (bright, very large single spike-evoked fluorescence transients, low glutamate-free fluorescence, kinetics similar to SF-iGluSnFR, more linear than SF-iGluSnFR) and iGluSnFR3.v857 (bright, large single spike-evoked fluorescence transients, very low glutamate-free fluorescence, kinetics faster than v82). Selectivity of iGluSnFR3 remained strong for glutamate over other amino acids and neurotransmitters (Fig. 3f).

Having dramatically improved the photophysical properties of the soluble sensor molecules, we next set about improving the quality of in vivo—and particularly synaptic—imaging. The first two generations of iGluSnFR traffic relatively well to the cell surface but nevertheless show some degree of accumulation of immature intracellular protein in intracellular organelles such as the endoplasmic reticulum and were revealed by high-resolution expansion microscopy to be excluded from the postsynaptic density [22]. We collected a battery of membrane-targeting sequences and signal peptides, attached them to the C- and N-termini, respectively, of iGluSnFR3.v82 and iGluSnFR3.v857, and tested sensors in cultured neurons for responses to spontaneous (single vesicle) release events ("optical minis"), selecting the best several combinations for further characterization. The final three variants selected include the terminus from the original iGluSnFR (from the pDisplay vector; the transmembrane helix from platelet-derived growth factor receptor, "PDGFR"), the GPI anchor sequence from the Nogo-66 receptor NgR1 ("NGR"), and a composite sequence from several motifs from the voltage-gated calcium channel accessory subunit Stargazin ("SGZ"). Choice of targeting sequence will depend on organism (note that species-specific targeting sequences are frequently required), cell type, imaging strategy, etc. In the future, it will be important to develop iGluSnFR variants that are specifically targeted to the pre- or post-synapse, among other key cellular locales.

7 Protocols for iGluSnFR Imaging in Several Preparations and Model Organisms

Each preparation for iGluSnFR imaging presents its own opportunities and challenges. In every prep, the sensor must be expressed sufficiently to yield good signal-to-noise ratio for imaging. However, overly strong expression levels produce excessive background fluorescence and could potentially buffer glutamate or otherwise alter neural circuit function [15, 17]. Targeting iGluSnFR specifically to synapses could dramatically decrease background fluorescence, ease signal segmentation, and lessen concerns of glutamate

buffering (although, as noted above, such targeted sensors have their own potential issues). Some preps are amenable to ready transgenesis at robust retargetable loci, such as *Drosophila* and its stable GAL4 and LexAOp lines [23, 24, 25]. Other preps offer convenient transduction through viral vectors, such as adeno-associated virus (AAV) in rodents. Some preps present multiple options for transduction but have no clear field-wide standard, such as worm and fish. Here we discuss notable aspects of iGluSnFR transduction, imaging, and interpretation in the most routinely used lab preparations including bacteria, tissue culture cells, and brain slices and model animals including worm, fly, fish, and rodents. The methods for transduction and imaging of iGluSnFR in diverse preps are essentially the same as those for GCaMP, albeit the localization of fluorescence changes to the membrane (as opposed to the cytoplasm for typical GCaMP imaging) presents additional hurdles for iGluSnFR imaging.

For the sake of clarity and conciseness, we focus on neurons, but iGluSnFR and other sensors are useful in glia and other cell types. Glutamate evolved as a signaling molecule in bacteria (as did ionotropic and metabotropic glutamate receptors), and its role has been preserved throughout billions of years of evolution across kingdoms.

7.1 Bacteria (Escherichia coli)

The bacterium *Escherichia coli* (*E. coli*) is the workhorse for producing recombinant protein of iGluSnFR (and other sensors, for that matter); there are also opportunities for studying the role of glutamate as a signaling molecule. *E. coli* is a fast-growing bacterium that is easily grown to high densities in simple culture media. *E. coli* offers several key advantages compared to other in vitro and in vivo methods discussed in this study, such as fast growth and high yield, low cost, and compatibility with high-throughput fluorescence spectroscopic and microscopic techniques. This allows for large-scale production of iGluSnFR protein in a relatively short time at a low cost. The general workflow of expressing iGluSnFR in *E. coli* is described in Fig. 4a.

First, a plasmid encoding the iGluSnFR gene in a bacterial expression vector is introduced into bacterial cells. This is often done through heat shock transformation where the plasmid encoding iGluSnFR is added to competent *E. coli* cells, and the mixture is subjected to a temperature shock, typically from ice-cold to a higher temperature (e.g., 42 °C), followed by a quick return to ice-cold conditions. This thermal shock promotes the uptake of DNA by the cells. After heat shock, the transformed cells are allowed to recover and then plated on selective media to isolate colonies containing the desired iGluSnFR gene. Another commonly used method is electroporation, where *E. coli* cells are subjected to an electric field, which transiently disrupts the cell membrane and allows DNA

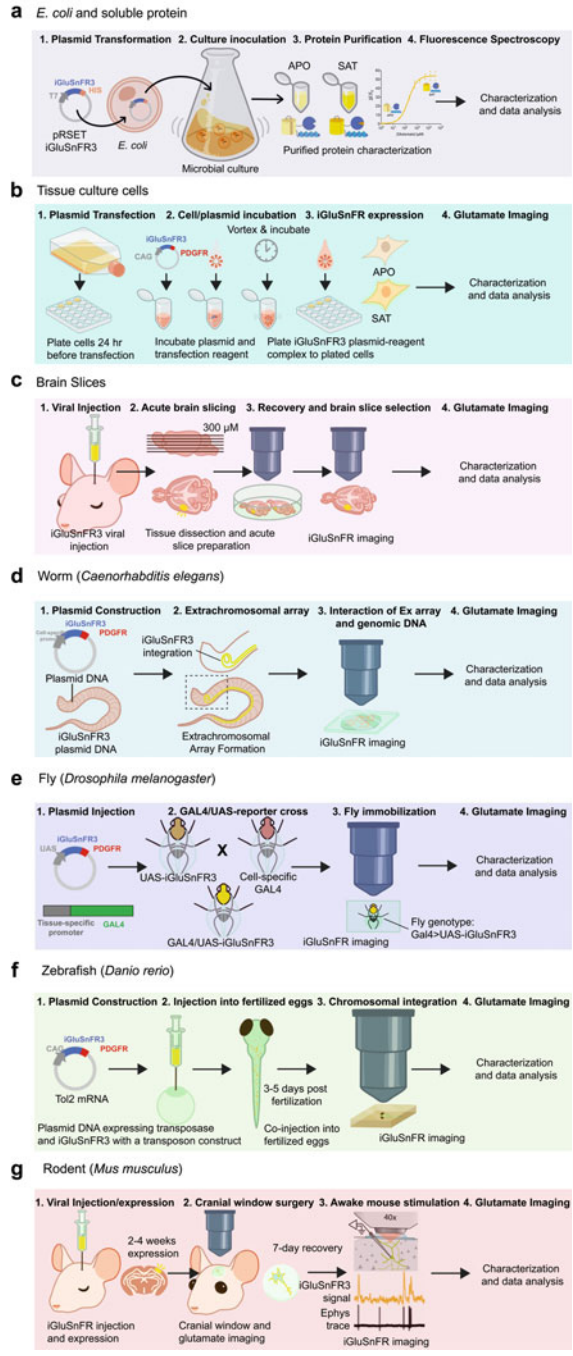

Fig. 4 Workflow for iGluSnFR imaging in several preparations and model organisms. General workflow for expressing and imaging iGluSnFR in various preparations and model organisms

uptake. Following electroporation, the cells are allowed to recover and then plated onto selective media for the isolation of transformed colonies.

Once a plasmid containing iGluSnFR gene is transformed into *E. coli*, it is allowed to express in a desired culture medium. First, the iGluSnFR gene is cloned into a bacterial expression system with a *lac* operon-based promoter, such as the T7 promoter/*lac* operator system in pET vectors. The T7 promoter/*lac* operator is tightly repressed in the absence of IPTG; IPTG relieves this repression, allowing the T7 promoter to initiate transcription and drive iGluSnFR expression. Another approach used is auto-induction media, which is a simplified and efficient approach for protein expression that automatically induces protein production without the need for monitoring or manual induction. This simple approach facilitates high-density cell cultures and often results in higher protein yields.

Once the protein has been expressed, bacterial cells are lysed to release the iGluSnFR protein. Several methods are used for bacterial cell lysis, such as physical, chemical, and enzymatic approaches. Common methods include mechanical disruption such as sonication to produce high-frequency sound waves to disrupt cell membranes or detergent lysis such as SDS or Bacterial Protein Extraction Reagent (BPER), where the cell membrane is disrupted, and the cellular components are solubilized. In some instances, bacterial cells can be subjected to repeated cycles of freezing and thawing. These freeze-thaw cycles cause ice crystals to form, leading to physical disruption of the cell membrane. Upon thawing, the cells rupture, releasing their intracellular components. The choice of cell lysis method depends on various factors, including the type of bacteria, the amount of protein desired, and the downstream applications.

Once the intracellular components have been extracted, the desired iGluSnFR protein is isolated and purified using His-tag protein purification. The iGluSnFR bacterial expression vector has a His-tag (a short stretch of histidine residues) added to the N-terminus of the plasmid. The purification process takes advantage of the specific binding of the His-tag to immobilized Ni^{2+} ions, attached to a purification column. This allows for a relatively simple and efficient way to purify iGluSnFR with high specificity. The extracted protein is then dialyzed to remove salts, detergents, and low-molecular-weight contaminations from the protein sample, resulting in a purified protein sample with the desired buffer composition and physiological pH. The protein concentration is then quantified and used for downstream applications and characterization.

iGluSnFR (and an iGluSnFR mutant specific for aspartate) has also been used to study the role of glutamate and aspartate as signaling molecules in *E. coli*, specifically as chemoattractants

[26]. In this preparation, purified iGluSnFR protein is added to the medium, with the resulting fluorescent transients revealing the gradient upon which individual bacteria are navigating.

If iGluSnFR is not expressing well in *E. coli* in your hands, first verify the construct by double-checking the DNA sequence and confirming that there are no unexpected mutations. In some instances, it can also be beneficial to optimize the codon usage of the gene to best suit it for the specific bacterial species or strain. Ensure that the growth conditions, including temperature, pH, and media composition, are optimal for the strain. If users are having difficulties expressing iGluSnFR, we recommend using a positive control to ensure that there are no issues with bacterial competent cells, transformation, and/or growth conditions. The user can also consider testing other *E. coli* strains, such as such as T7Express (NEB) or BL21 (NEB), to see if the issue is strain-specific. If the protein expresses but the yield is low, we recommend shaking at 37 °C with ample aeration to enhance protein expression. Induction during the early exponential phase may also lead to higher protein yield compared to induction at later stages. Additionally, controlling cell density by adjusting the inoculation density or using fed-batch culture techniques can optimize protein expression levels. Empirically, we have found that iGluSnFR3 (and earlier variants of iGluSnFR) also express extremely well in *E. coli* when grown in 500 mL or 1 L of culture and shaken at 30 °C in auto-induction media for 36–48 h.

7.2 Tissue Culture Cells

Tissue culture cells are widely used in a wide range of research areas. They are readily available and can be obtained from cell culture repositories, making them convenient for expressing and studying glutamate dynamics using iGluSnFR in a human cell line. Tissue culture cells offer some advantages over the in vivo systems explained below—they have a rapid proliferation rate, allowing for quick and efficient protein expression experiments, and their ability to rapidly divide and generate large cell populations makes them suitable for medium-throughput studies or large-scale protein production if needed. They have also been extensively characterized over the years, and this knowledge base facilitates experimental design, troubleshooting, and comparisons with other studies. Being a eukaryotic system, tissue culture cells provide a more native eukaryotic intracellular environment for testing sensor function. This enables us to study iGluSnFR and glutamate dynamics in an environment that requires proper folding, posttranslational modifications, and functional activity specific to eukaryotic systems.

The cells are maintained in appropriate growth medium (e.g., DMEM supplemented with FBS and antibiotics) and incubated in a suitable cell culture incubator at 37 °C with 5% CO_2 until they reach approximately 70–80% confluence. An appropriate transfection reagent is used for delivering the plasmid into the cells.

Examples of commonly used transfection reagents include liposomal-based reagents (e.g., lipofectamine), calcium phosphate, or electroporation. The choice of reagent depends on factors such as cell type, transfection efficiency, and toxicity.

To transfect, first the plasmid DNA and the transfection reagent are diluted in Opti-MEM or serum-free medium (Fig. 4b). The two tubes are intubated for 5–10 min at room temperature. Next, the diluted DNA is combined with the diluted transfection reagent, gently mixed, and incubated for an additional 15–30 min at room temperature. This process allows the formation of transfection complexes. Finally, the transfection mix is added dropwise to HeLa cells in a culture dish or plate containing the growth medium and gently swirled to ensure uniform distribution. The cells are incubated with the transfection mix typically for 4–7 h while being kept in a suitable environment at 37 °C with 5% CO_2. After the incubation period, the transfection mix is removed and replaced with fresh growth medium containing serum. The cells are allowed 3–5 days to recover and express iGluSnFR3 protein.

After expression, the cells can be used to perform downstream applications and assays, such as fluorescence microscopy in the presence and absence of glutamate, or advanced imaging like expansion microscopy or electron microscopy. These assays further help validate the expression and localization of iGluSnFR3 and help researchers study glutamate dynamics in cells.

If you are not observing any iGluSnFR expression in tissue culture cells, there are several potential issues to check first. First, verify transfection efficiency by checking if the cells are successfully transfected with the iGluSnFR construct; you can amplify signal with anti-GFP antibodies if signal is low. Ensure that you are using an appropriate transfection method and optimize transfection conditions such as DNA-to-reagent ratio, incubation time, transfection method, or the use of transfection enhancers. Confirm that the construct is intact and free of any mutations that could affect its expression. Next, evaluate the choice of promoter and ensure it is suitable for driving expression in your specific cell line. In many instances, the viral *CAG* promoter will give strong expression. For excitatory neurons, *hSynapsin-1*, *CaMKII*, or *EF1α* may work well; for inhibitory neurons, the *mDlx* enhancer may work well. For astrocytes, the *GfaABC$_1$D* promoter may work well. Evaluate the culture conditions, including the growth medium, temperature, pH, and gas exchange. Ensure that the cells are maintained under optimal conditions for growth and viability. Inadequate culture conditions may affect the efficiency of transfection, subsequent protein expression, and cell health and function. You may also need to optimize imaging conditions such as exposure time, illumination intensity, excitation wavelength, and filters to maximize the detection of iGluSnFR fluorescence. Finally, confirm that you are leaving sufficient time for protein synthesis, accumulation,

targeting, and chromophore maturation. In our experience, it usually takes 2–4 days to see iGluSnFR3 expression in HeLa or HEK293 cells.

7.3 Brain Slices

Acute brain slices maintain the three-dimensional structure and cellular organization of brain tissue, providing a more physiologically relevant environment compared to tissue culture cells or tissue homogenates. They also preserve the functional properties of neurons and glial cells, including their intrinsic electrical activity, synaptic connectivity, and receptor expression. This allows for the study of intact neuronal circuits, cellular interactions, and network activity and the investigation of glutamate synaptic transmission under near-physiological conditions.

Preparing acute brain slices involves several key steps, including brain extraction, slicing and recovery, and selection of suitable brain slices expressing iGluSnFR for downstream applications (Fig. 4c). Prior to brain injection, iGluSnFR3-expressing AAV is injected into the brain region of interest. The protein is allowed to express for 2–4 weeks in the target cells before brain extraction. Next, the brain is removed from the skull of an anesthetized rat using sterile techniques and in accordance with approved animal protocols and ethical guidelines. The extracted brain is placed in ice-cold, oxygenated artificial cerebrospinal fluid (ACSF) that matches the composition appropriate for the brain region of interest. Then, using a vibratome or a microtome, brain slices are cut to the desired thickness (typically 300 microns) in the appropriate orientation (coronal, sagittal, or horizontal).

The brain slices are transferred to a holding chamber or culture dish containing oxygenated ACSF at 37 °C, allowing the slices to recover for at least 1 h. This recovery period allows the brain slices to stabilize and regain normal physiology. Once the recovery period is complete, brain slices expressing iGluSnFR3 are identified using a fluorescence microscope. The intact and healthy-looking slices that exhibit strong iGluSnFR3 fluorescence are used for downstream applications and characterization.

If the user is not seeing any iGluSnFR expression in brain slices, there are several potential issues to check first. First, confirm the efficiency of the AAV prep used to introduce iGluSnFR into the brain slices. Optimize delivery parameters, such as plasmid concentration or viral functional titer, incubation time, and penetration depth, to enhance delivery efficiency. Check the integrity and quality of the iGluSnFR construct. Verify the DNA sequence and confirm that it is intact and free of mutations that may affect its expression. Evaluate the choice of promoter used to drive iGluSnFR expression in brain slices, in your cell type(s) of interest. Certain promoters may have limited activity in specific brain regions or cell types. Consider using a promoter that is well characterized and known to be effective in the target brain region. Finally, consider using positive controls such as other biosensors,

fluorescent markers, or proteins known to be expressed in brain slices. This will help determine if the issue lies specifically with iGluSnFR or if there are general challenges with protein expression or detection in the brain slice preparation.

If using viral vectors, ensure that the viral particles are functional and have not undergone any degradation during storage or handling. AAV particles can be sensitive to freeze-thaw cycles, so aliquot into small amounts for single use. AAV infection efficiency can be sensitive to contaminants such as residual cesium chloride from particle purification; some batches have low efficiency for reasons that remain unknown. We encourage testing virus preparations from multiple sources. Isolate viral DNA from particles and run it on a gel and PCR and/or sequence it to determine if there are contaminating constructs, if the construct has mutations, or if Cre-dependent (or other recombinase-compatible) constructs have undergone recombination.

7.4 Worm (*Caenorhabditis elegans*)

The worm preparation offers several key advantages, including small size, known connectivity, and optical transparency. Characterizing and using biosensors in the worm allows researchers to investigate biological processes and phenomena within the context of a living organism. They allow for a more comprehensive analysis of the underlying genetic, neural, and environmental factors that influence behavior. In contrast, *E. coli*, cell cultures, and brain slices offer limited behavior observations. Worms also have a relatively short life span of a few weeks, which makes it suitable for expressing a wide range of biosensors in a short time frame. Overall, worms offer the advantage of an intact organism, allowing researchers to investigate glutamate dynamics in a broader range of biological processes and behaviors.

For relatively quick expression of transgenes, DNA plasmid constructs can be microinjected into germline cells to generate "transient transgenic" progeny expressing stable extrachromosomal arrays (Fig. 4d). A comprehensive guide for transformation of strains via DNA microinjection is available on Wormbook [27, 28]. While stabilization of lines can be achieved in as little as 14 days, there are caveats to using extrachromosomal arrays for generating iGluSnFR-expressing strains. Notably, extrachromosomal array expression levels are quite variable between individuals, making comparisons between imaging experiments problematic. There is also variability in copy number and expression of constructs introduced via germline transformation [27, 28]. Since the resulting transformants are genetic mosaics, constructs are inherited in a non-Mendelian fashion. These inherited arrays are also subject to recombination and truncation of gene fragments.

While extrachromosomal arrays are generally sufficient for iGluSnFR expression and qualitative evaluation of glutamate transmission dynamics at nematode synapses, genomic integration of

iGluSnFR constructs is an option to ensure stability of strains and to facilitate quantitative imaging experiments. A straightforward solution to the issues presented by microinjection is targeted, single-copy insertion of the transgene. Optimization of CRISPR has made it more amenable to the nematode system for genome editing. Another genome editing tool, MosSCI (Mos1-mediated Single Copy Insertion), has also been used to generate transformants [29, 30, 31]. Erik Jorgensen's lab developed MosSCI by introducing the Mos1 transposon from *Drosophila* into the *C. elegans* system. Mos1 excision-induced transgene-instructed gene conversion (MosTIC) relies on the presence of the Mos1 insertion at a specific genetic locus for editing to occur. Additionally, the Nematode Gene-Tagging Tools and Resources Consortium (NemaGENETAG) has generated a large strain library with Mos1 insertions across different chromosomal loci. This resource and strains can be obtained through the Caenorhabditis Genetics Center (CGC), and published plasmids can be obtained through Addgene.

The optical transparency of the nematode allows for easy visual access of the internal anatomy while bypassing the need for surgery. This enables in vivo imaging of sensors and structural markers in neurons, glia, and other cell types. iGluSnFR recordings can be captured through confocal or two-photon microscopy. In some cases, depending on the region of interest and the events being captured, a simple epifluorescence imaging setup may be sufficient. Depolarization of *C. elegans* neurons typically occurs over the span of seconds, much longer than the millisecond-scale action potentials of mammalian neurons. As such, fast imaging speeds are not necessary to capture neuronal glutamate transients. Imaging speeds ranging from a few frames per second to even 1 fps are sufficient.

PDMS (polydimethylsiloxane) microfluidic chips offer stable environments for capturing neuronal responses to a range of chemical stimuli [32]. Controlled introduction to stimuli is also possible under a variety of conditions, depending on the design of the chip: some have microchambers designed to snugly fit worms and are designed so that only the amphid neurons of the trapped worm are stimulated during timed exposure to stimuli; other chips are more complex and allow for locomotion of the worm as it navigates a chemical gradient [33, 34, 35]. For further restriction of animal movement during imaging, worms can be paralyzed with levamisole or tetramisole solution [36, 37, 38].

Previous work in the Bargmann lab has validated that the synaptic glutamate inputs detected by iGluSnFR in the *C. elegans* nerve ring are indeed glutamatergic and presynaptic in origin [16]. Simultaneous imaging of iGluSnFR and the red genetically encoded calcium indicator RCaMP in *C. elegans* AVA neurons reveal that iGluSnFR responses reliably precede RCaMP signals (up to several seconds in advance), consistent with previous

findings that glutamate provides strong excitation of AVA [16]. Patterns of spontaneous glutamate release also correlate with oscillatory calcium activity of AVA during locomotion [39]. iGluSnFR was also found to be strongly localized to AVA neuronal processes in the nerve ring, and glutamate transients on these neuronal processes are easily distinguishable from the cell body during imaging [16]. While iGluSnFR has been recorded extensively in AVA, iGluSnFR studies have very recently expanded to include other neurons and circuits. These studies include interneurons such as AIB (unpublished data) and AIY [40] (which are both members of AWC and ASE chemosensory circuits) and second layer interneurons like RIB [41].

In addition to the troubleshooting steps discussed above, evaluate the timing and developmental stage of worms during transgene expression. iGluSnFR expression may be developmentally regulated or specific to certain cell types or tissues. Ensure that you are examining the worms at the appropriate developmental stage or time point for iGluSnFR expression in your cell(s) of interest. Optimize the culture conditions of the worms. Ensure that they are maintained under suitable conditions, including temperature, humidity, and nutrient availability. *C. elegans* requires specific culture conditions for optimal growth and gene expression. Suboptimal culture conditions can affect overall health and the ability to detect iGluSnFR expression. iGluSnFR typically (and surprisingly) expresses well with the secretion leader peptide (from Igκ) and membrane helical anchor (from PDGFR) from the pDisplay mammalian vector. It is possible that some cell types and conditions will instead require the use of targeting sequences from worm.

7.5 *Fly (*Drosophila melanogaster*)*

Fruit flies (*Drosophila melanogaster)* are another widely used model organism and present a more complex system than worms, bacteria, or brain slices. Flies have stereotyped brains and nerve cords and a robust behavioral repertoire. Flies use glutamate at their neuromuscular junction and at ~1% of adult synapses (acetylcholine instead being the dominant excitatory neurotransmitter). Flies are optically accessible in embryonic and larval stages, although the adult is covered by a highly pigmented cuticle that complicates imaging. Many biological processes and pathways are conserved between fruit flies and humans, making fly a good model organism for studying glutamate dynamics using iGluSnFR.

For expression of iGluSnFR, as with expression of other exogenous gene sequences, the GAL4/UAS or LexAOp systems can be used to drive robust, tissue-specific expression [23, 24, 25]. Several strains containing iGluSnFR under the control of UAS enhancer have already been generated using transposon-mediated transgene insertion and are readily available through the Bloomington Stock Center (made by the Looger lab and deposited by Stefan Pulver, 2015; #59609-59613).

The translucent cuticle allows for structures as fine as dendrites to be imaged in *Drosophila* larvae without surgery. Additionally, many larval tissues are polyploid and very large, facilitating visualization of subcellular processes [42]. Preparation of larvae for iGluSnFR imaging has several considerations both to reduce lethality and improve imaging quality during recording. Immobilization can be achieved with a setup as simple as gently squeezing live larvae in halocarbon oil under a glass coverslip [43, 44]. Alternatively, PDMS microfluidic chips with specialized microchambers to fit different larval and embryonic stages can provide consistent vacuum-applied pressure, gently restraining animals without anesthesia [45]. However, both methods for long-term time-lapse imaging of live animals can prove challenging without dissection, which can prove fatal. Anesthetics for larval imaging include cold temperature and carbon dioxide (CO_2) [46], in addition to chemicals such as chloroform, isoflurane, desflurane, and diethyl ether [42, 47, 48], though anesthetics have been shown to alter behavior and/or physiological activity and even decrease viability [42, 45, 49]. Alternatively, adhesives can be used for partial immobilization of *Drosophila* across all larval stages for imaging. However, adhesive-based immobilization can be toxic to animals and irreversible, as animals cannot be retrieved after adhesion to coverslips [45]. Stability and survival of larvae can be prolonged by using a combination of these techniques; for example, LarvaSPA (Larva Stabilization by Partial Attachment) allows for continuous imaging for periods longer than 10 h through combined application of UV-based glue for partial attachment to a coverslip and a PDMS block to further restrain larval movements (in addition to retaining air and moisture) [50].

Imaging of adult flies is complicated by the fact that surgery must be performed to gain access to neurons for imaging. The cuticle (much darker in adults than larvae) significantly degrades imaging quality, particularly in deep regions; it can be cut away with tools such as hypodermic needles, razor blades, and forceps [51, 52]. The choice of anesthetics for adult flies is the same as larvae, and adults can also be immobilized with adhesive for imaging. After cuticle removal, flies quickly begin to desiccate, particularly under bright illumination; it is imperative to maintain adequate imaging buffer above the cuticular hole.

For capturing iGluSnFR signals in *Drosophila*, spinning-disk confocal microscopy may be well suited due to fast imaging speeds and minimal photobleaching. Kakanj et al. provide an excellent guide on long-term in vivo imaging of *Drosophila* larvae and adults [42, 43]. A particular challenge of long-term imaging of subcellular events in *Drosophila* (such as the subcellular localization of glutamate signals) is the stress induced by constant illumination (both through phototoxicity and activation of photoreceptors), which can be partially mitigated by the use of spinning-disk illumination.

An even better option might be light-sheet imaging, which further reduces photobleaching and out-of-focus light. Light-sheet imaging is compatible with larvae, where GCaMP has been imaged to great success [53], whereas adult flies do not obviously provide optical access.

However, for simple short-term imaging of iGluSnFR, simple confocal microscopy is sufficient and can be further optimized with airyscanning. Two-photon imaging allows for tighter restriction of excitation light and better penetration of tissues (such as the adult cuticle), but at the cost of more expensive rigs, slower volume scan rates [54], and sometimes severe brain heating. Previous studies indicate that glutamate events can be imaged at the scale of hundreds of milliseconds [44, 54], though some events (such as responses in the visual system) may be optimally captured in the millisecond range [51]. The general workflow is described in Fig. 4e.

In addition to the troubleshooting tips shared for other preparations and animals, verify that imaging parameters used to detect iGluSnFR fluorescence in flies are appropriate. Adjust the exposure time, laser intensity, and filters to optimize the detection of the fluorescence signal. Consider using confocal microscopy or specialized imaging techniques for better resolution and signal-to-noise ratio. We found that the Igκ secretion leader peptide from the mammalian expression vector produced no obvious iGluSnFR expression in flies. The version that we made and deposited at Bloomington has the secretion leader peptide from *Drosophila* heat shock protein 70 (*a.k.a.* binding immunoglobulin protein, BiP) in place of the Igκ leader. This line has produced robust fluorescent signals in diverse *Drosophila* experiments [51, 52, 55, 56]. It may be worthwhile to modify the iGluSnFR construct by incorporating different secretion peptides and transmembrane anchors and screen for ones that effectively target iGluSnFR in flies.

7.6 *Zebrafish* (Danio rerio)

Zebrafish is another model organism that offers several advantages for studying glutamate dynamics using iGluSnFR. Zebrafish provides greater relevance for mammalian (and human) neuroscience than flies, worms, and bacteria and as an intact organism will yield more robust discoveries about glutamatergic signaling than cultured cells and brain slice. Zebrafish exhibits a wide range of complex behaviors that rely on glutamatergic signaling, including locomotion, feeding, learning, memory, and responses to sensory stimuli. Zebrafish is quite transparent in the embryonic and young larval stages. This transparency and relative ease of transient transgenesis make zebrafish amenable to medium-throughput testing of fluorescent variants, enabling rapid assessment of fairly large numbers of iGluSnFR variants. It should be noted that expression levels and patterns are quite variable in transient transgenics and, as such, this screening would be mostly qualitative in nature.

The most used transduction method in zebrafish involves microinjection of single-cell embryos with a plasmid DNA construct, along with mRNA and/or protein of a transposase, often Tol2 (Fig. 4f). Transposon-mediated transgenesis also allows for introduction of Cre/LoxP or GAL4/UAS constructs for inducible expression. This method was used [57] to generate strains expressing glia-specific iGluSnFR. Tol2-mediated transformation is further facilitated by the Tol2kit system, which utilizes site-specific recombination-based cloning to overcome obstacles such as low transgenesis efficiency and difficulty tracking successful germline integrations without the use of fluorescent marker transgenes [58].

In addition to the ease of obtaining constructs and reagents in the Tol2kit system, the zebrafish system also benefits from optical transparency of the animals in the larval and embryonic stages (often increased by mutation of pigmentation genes) [59, 60]. This provides easier access for imaging at the level of the whole brain or individual neurons without the need for surgery. iGluSnFR signals can be captured at several hundred frames per second [57, 61]. Two-photon microscopy has been commonly used to record iGluSnFR signals in the zebrafish system [57, 61, 62].

For intact, in vivo imaging of zebrafish, whole-body and site-specific immobilization is recommended. Larvae can be embedded in low melting-point agarose (typically 3%) and mounted on a glass slide [57]. Additional immobilization can be achieved through site-specific injection of α-bungarotoxin, as used by [57] (microinjections of 2 mg/mL concentration) for ocular muscle paralysis. Direct microinjection of 125 μM α-bungarotoxin into the heart can also suppress whole-body movement [61]. Tricaine methanesulfonate (MS-222) can be used for deeper anesthesia should surgery or absolute stillness be required for iGluSnFR imaging. In one comparative study of anesthesia techniques, adult zebrafish exposed to MS-222 were not found to display stress-related behaviors during induction or recovery, nor was there anesthesia-induced death during anesthesia or in the 14-day period after [63]. For larval imaging, embryo media containing 0.02% MS-222 solution can be added to recording chambers for immobilization and mounting prior to imaging [64]. Imaging of larvae in media may be preferable for following neuronal glutamate responses to chemical stimuli or odorants, which can be introduced directly into the recording chamber.

When troubleshooting a lack of expression in zebrafish, check the integrity and quality of the iGluSnFR construct (GAL4/UAS or direct promoter fusion, etc.). Confirm that the DNA sequence is intact and free of mutations that may affect its expression. Confirm that the Tol2 transposase is active and functional. Prepare the transposase enzyme according to the recommended protocols and confirm its activity using appropriate control reactions. If the

transposase activity is compromised, this may result in reduced or no integration of the iGluSnFR construct. Check the integrity and quality of the Tol2 transposon vector carrying the iGluSnFR construct. Verify that the vector was properly prepared, purified, and stored. The ratio of Tol2 transposon vector to transposase can influence integration efficiency. Ensure that the iGluSnFR mRNA is of high quality and accurately quantified. Verify that mRNA synthesis was carried out correctly and that there was no degradation or contamination during synthesis or storage. Perform control experiments to evaluate the functionality of the Tol2 transposase and the iGluSnFR construct and to ensure that nothing is going wrong with your microinjections.

7.7 Rodent (Mouse, Mus musculus)

Rodents are extensively used as models for various human diseases, including neurodegenerative disorders, psychiatric disorders, and neurological conditions involving aberrant glutamate dynamics. They are the most commonly used model organisms in the lab due to their genetic and physiological similarity to humans, complex nervous system, behavioral repertoire, and suitability for pharmacological studies. Their brain structure, including glutamatergic synapses and signaling, is more similar to humans than flies, worms, or zebrafish. Rodents exhibit a rich repertoire of behaviors, including learning, memory, social interactions, and sensorimotor responses. Many of these behaviors involve glutamate signaling and can be modulated by changes in glutamate dynamics. Studying glutamate dynamics in the context of rodent behavior allows for a more comprehensive understanding of the functional consequences of glutamate signaling in complex neural circuits. Overall, rodents provide an important platform for assessing glutamate dynamics using iGluSnFR.

The expression of iGluSnFR in rodent typically involves the use of stereotactic apparatus and careful surgical techniques. Briefly, expression can be conveniently produced using stereotactically injected adeno-associated viral (AAV) particles expressing the iGluSnFR gene (Fig. 4g). First, the mouse is anesthetized using a suitable anesthesia protocol, such as intraperitoneal injection of an anesthetic agent like ketamine and xylazine, or isoflurane inhalation anesthesia. Then, the anesthetized mouse is placed onto a stereotactic frame to immobilize the head during the surgery. Next, the surgical area is typically shaved and cleaned with a disinfectant solution.

Once the surgical area has been exposed, a small incision is made in the skin at the intended injection site, exposing the underlying tissue. The stereotactic coordinates for the target brain region are determined. Next, a small hole is drilled into the skull using a dental drill or a micro-drill. Care is taken to avoid damaging the

underlying brain tissue and to ensure the proper depth of the hole. Once the hole is created, the injection needle or pipette is slowly lowered into the brain to reach the target region.

The AAV particles containing iGluSnFR are then infused into the brain using a microinjector. The injection is typically performed at a controlled rate to allow for gradual diffusion of the virus within the target area and to avoid unnecessary tissue damage. After the infusion is complete, the pipette is slowly withdrawn, and bleeding is controlled using sterile techniques. The exposed brain tissue is typically covered with a transparent sealing material, such as a glass coverslip or a custom-made coverslip with an optical adhesive. The sealing material is carefully positioned and secured to create an optical interface for imaging while maintaining the stability and integrity of the brain tissue.

After the cranial window is installed, the incision is closed using sutures or wound clips. The animal is closely monitored during the recovery period and provided with suitable postoperative care, including warmth, hydration, and any necessary postoperative medication. It is monitored regularly for expression and imaged using a fluorescent microscope.

When troubleshooting a lack of iGluSnFR expression in rodents, confirm the AAV's integrity through sequencing, ensuring that the iGluSnFR gene is intact. Optimize the delivery parameters, such as the titer of the virus, the viral promoter, the incubation time, the serotype of the AAV, and animal handling and sample preparation procedures. Consider the time point at which you are examining the rodents. Ensure that you wait sufficiently long (2–3 weeks is typical) for robust expression from the AAV. It may also be worthwhile to test different anchoring domains. In our experience, some anchoring domains (e.g., GPI anchor and PDGFR transmembrane domain) express and traffic better than other domain (e.g., SGZ domain). Genetic background can further influence transgene expression in rodents. Test the construct in different genetic backgrounds to determine if expression is strain-dependent. Additionally, account for biological variability by using an adequate sample size and considering statistical analysis to assess expression differences among individuals.

Other expression methods are used, as well. In utero electroporation can produce adequate sensor expression levels. Notably, transgenic lines expressing iGluSnFR have been used to great success. The best characterized line is B6;129S-Igs7tm85.1(tetO-gltI/GFP*)Hze/J (Jackson Labs #026260), which expressed the first-generation iGluSnFR in a Tet-dependent fashion. This line has been used for several notable studies of glutamatergic signaling in mouse [65–69].

8 In Vivo Functional Imaging of iGluSnFR3 Using Two-Photon Laser Scanning Microscopy

We regularly image iGluSnFR expressed in the mouse cortex using stereotactically injected AAV particles. Here, we describe briefly our protocol for expressing iGluSnFR in the mouse cortex along with a snippet of our unpublished results. First, we achieved sparse and bright expression of iGluSnFR using a mix of low-titer (5E8 GC/mL) AAV1-*CaMKII*-Cre and high-titer (5E12 GC/mL) AAV9-*hSyn*-FLEX-iGluSnFR3.v857.GPI viruses. To prevent viral particle aggregation and adsorption to plastic surfaces, the viral dilutions from stock and aliquot storage were done in a buffer containing 1X PBS supplemented with 35 mM NaCl, 5% glycerol, and 0.001% Pluronic F68 (Thermo Fisher).

Two-month-old mice (C57/BL6J) were placed under isoflurane anesthesia, and a 5 mm diameter craniotomy was made above the left hemisphere visual cortex area V1 (Fig. 5a). Following durotomy, 100 nL viral mix was injected using a beveled glass micropipette, targeting layer 2/3 pyramidal neurons at AP −4.0 mm, ML −2.8 mm, and DV −0.3 mm and at a second location (AP −2.5 mm). Subsequently, the craniotomy was sealed with a glass coverslip, and a headbar was glued to the skull for performing head-fixed two-photon laser scanning microscopy [70].

Functional imaging was performed on a custom-built two-photon laser scanning microscope, SLAP2 (an improved version of SLAP microscopy [21]), which uses raster scanning two-photon imaging at 1030 nm excitation to image two separate locations on

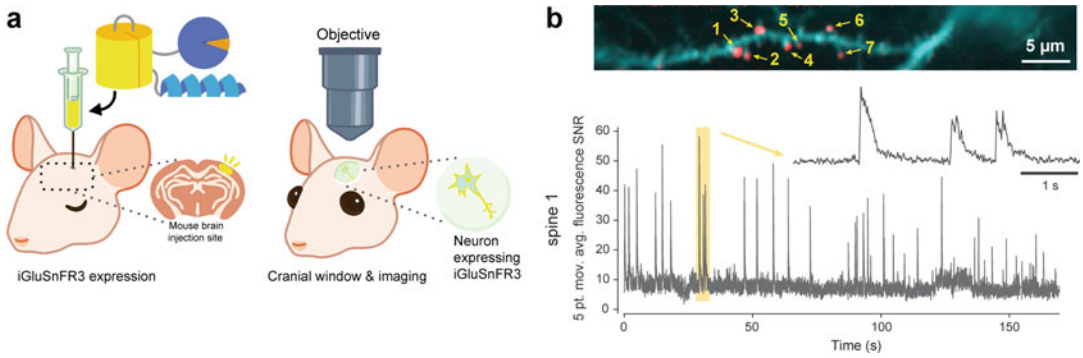

Fig. 5 Glutamatergic imaging of cortical synaptic activity in awake mice using iGluSnFR3. (**a**) Schematic of stereotactic viral injection and cortical imaging. (**b**) Glutamatergic imaging of cortical synaptic activity in awake mice. Image inset shows a V1 visual cortex layer 2/3 pyramidal neuron basal dendrite labeled with iGluSnFR3.v857 (cyan) and active synapses (red) marked by pixels with high local correlated activity. One example recording without bleaching correction, sampled at 261 Hz, and using a five-point moving average is shown for fluorescence collected from the active (red) zone of spine 1. High-SNR synaptic events are clearly distinguishable over the entire 3-min recording, despite bleaching reducing fluorescence to about 70% from starting levels

the dendritic tree. Such a dual-plane imaging system is especially useful when combining glutamate imaging with postsynaptic visualization of calcium responses using, e.g., the genetically encoded red calcium sensor jRGECO1a [71] to study local dendritic Ca^{2+} spikes vs. global backpropagating action potentials.

At 3 weeks postinjection, viral expression levels were sufficiently high to detect glutamatergic activity over 3 min of recording time in awake behaving mice (Fig. 5b). To improve recording quality, it is essential to minimize movements by, e.g., optimizing surgical technique for imaging window implantation, head fixation equipment, and habituating the mouse to the setup. This is especially important for out-of-focus movements, since in-plane movements can be readily corrected using cross-correlation-based algorithms. In addition, it is important to optimize two-photon excitation laser power, viral expression levels, recording duration, and laser beam dwell time, such that glutamatergic events can be measured over time periods relevant to animal behavior. Too high excitation power, while initially yielding high-SNR events, would quickly bleach the sensor and limit the recording duration and the range of relevant animal behaviors. High excitation power, and long imaging sessions, can also lead to local brain heating and spurious neural activity [72]. Conversely, too low excitation power would permit extended recording times, but with SNR too low to confidently resolve synaptic events. With iGluSnFR3, the photostability and brightness under two-photon excitation are sufficiently good to continuously image for >3 min, which can be done repeatedly after allowing 5–10 min for unbleached sensor to diffuse across the branch.

9 Future Optimization of iGluSnFR

While iGluSnFR has greatly advanced our understanding of glutamate signaling, it still has headroom for optimization and diversification. Having developed the original iGluSnFR (2013), SF-iGluSnFR (2018), and now iGluSnFR3 (2023), we believe that gains can still be made in several sensor properties. There is also a pressing need for variants in other color channels, to permit multi-color imaging, simultaneous imaging and optogenetics, and deep imaging with red-shifted indicators. Further rounds of directed evolution, protein engineering, and high-throughput screening can improve both iGluSnFR and to-be-developed color variants.

9.1 Temporal Resolution

A critical avenue for improvement is to speed up the sensor's ON kinetics. Glutamate release into, and clearance from, the synaptic cleft is remarkably fast (<1 ms)—as such, sensors with fast ON kinetics are essential for accurate determination of the rapid rise (and fairly rapid fall) in glutamate concentration during synaptic

transmission. Indicators with slow ON kinetics will exhibit a delayed and prolonged response to changes in glutamate concentration. Such indicators cannot distinguish between synaptic and spillover glutamate, they cannot resolve trains of fast events, and they are more likely to buffer glutamate, thus interfering with the processes under study.

9.2 Saturation of Activation Kinetics

It is also important to reduce the saturation of iGluSnFR's activation kinetics during rapid, high-concentration bursts. The glutamate concentration that half-saturates ON rates, K_{fast}, is distinct from K_d, the concentration that half-saturates steady-state fluorescence. Indicators with low K_{fast} will saturate during large release events and be unable to distinguish any further release. As local glutamate concentrations can be extremely high in the confines of the synaptic cleft—and perhaps even more so in cleft microenvironments such as near the center of the active zone—indicators with higher K_{fast} will be critical for high-resolution determination of glutamate release and reuptake. Indicators with high K_{fast} will also help further discriminate synaptic from spilled-over glutamate.

9.3 Sensitivity and Dynamic Range

Another avenue to consider is expanding the dynamic range (the range of glutamate concentrations over which the sensor provides useable signal) and fluorescence change ($\Delta F/F_0$) upon binding to glutamate. A broader dynamic range will allow iGluSnFR to detect both subtle and large changes in glutamate levels. Having a higher $\Delta F/F_0$ will help distinguish the specific glutamate signal from background noise and other interfering factors. Improving both dynamic range and $\Delta F/F_0$ will improve the signal-to-noise-ratio, making it easier to differentiate between changes in glutamate concentration and any potential artifacts or background noise. Improvements in $\Delta F/F_0$ may come from rational design or directed evolution, to introduce mutations that increase the sensor's conformational change or saturated fluorescence or decrease resting fluorescence.

9.4 Photostability

Another important consideration for improving iGluSnFR is improving its photostability to minimize photobleaching due to prolonged or intense illumination. Having an indicator with improved photostability will allow for longer imaging sessions without significant loss of fluorescence signal. In general, photobleaching can introduce artifacts and distort the fluorescence signal, making quantification and analysis difficult. An indicator that is more photostable will enable sensitive and reliable detection of changes in glutamate concentration, particularly in low-level signal conditions or when monitoring subtle variations in glutamate dynamics. Improvements in photostability may come from introducing mutations close to the chromophore to decrease production of reactive oxygen species and/or increase the resistance of the

chromophore. A complementary approach is to improve the folding and thermodynamic stability of the sensor, making the indicator more resistant to misfolding and degradation caused by prolonged exposure to light.

9.5 Nanoscopic Localization

The earlier generations of iGluSnFR (iGluSnFR and SF-iGluSnFR) solely used the PDGFR transmembrane domain as a membrane-targeting domain. Our earlier experiments (not discussed here) suggested that PDGFR, when fused to iGluSnFR, resulted in poor nanoscopic localization at post-synapses. In addition to PDGFR, other membrane-targeting domains can be explored to achieve an improved nanoscopic localization to post-synapses. For example, in iGluSnFR3, a GPI (glycosylphosphatidylinositol) anchor has been used as an alternative membrane-targeting strategy. The GPI anchor in iGluSnFR provides improved surface expression, improved nanoscopic localization, and broad applicability in cell cultures and model organisms. While PDGFR has been widely used and validated as a membrane-targeting domain for iGluSnFR, other anchoring domains such as GPI anchors may offer an alternative that can provide improvements in membrane targeting, nanoscopic localization, and protein stability.

9.6 Fluorescent Protein Scaffold

Further improvements may also arise from incorporating new fluorescent proteins into iGluSnFR. The original iGluSnFR and the most widely used SF-iGluSnFR variant (SF-iGluSnFR.A184V) are both GFP-based sensors, and the more recent iGluSnFR3 is a mVenus-based sensor with an SYG chromophore. While other fluorescent proteins have been explored (e.g., mApple for a red iGluSnFR^{ncp} [18] and mAzurite for a blue-shifted iGluSnFR [73]), they have not been widely adopted due to poor performance. Leveraging the favorable properties of other fluorescent proteins can provide significant benefits for glutamate imaging. For example, certain fluorescent proteins (FPs), such as mNeonGreen or mScarlet3, exhibit high brightness and quantum yield. Utilizing these FPs might improve sensitivity and detection of iGluSnFR, particularly in low-expression or dimly labeled samples. Other fluorescent proteins, such as mTurquioise2 or mCerulean, have faster maturation kinetics. Using these FPs may help iGluSnFR mature and express functional protein on a faster timescale. Other fluorescent proteins show improved photostability [74]. By utilizing such photostable fluorescent proteins, glutamate sensors could be more resistant to photobleaching and maintain their fluorescence intensity over extended imaging periods. Finally, by employing different colored FPs, such as green-, red-, or blue-shifted FPs, researchers can perform multiplexed experiments, imaging glutamate in multiple cell types, or glutamate alongside other analytes.

9.7 Cooperative Behavior

A final property of iGluSnFR to adjust would be its degree of cooperativity. As presently constituted, each molecule of iGluSnFR binds a single glutamate (i.e., cooperativity = 1). The calcium sensor GCaMP is built upon the calmodulin Ca^{2+}-binding protein, which binds four Ca^{2+} ions per protein molecule. GCaMP sensors tend to be fairly cooperative, with Hill coefficients typically between 2 and 3.5 (less than 4, as binding of several Ca^{2+} ions may be sufficient to produce a fluorescence change, despite incomplete occupancy). The advantage of cooperative sensors like GCaMP is that they can transduce small changes in analyte concentration into large fluorescent changes. Downsides include typically smaller dynamic ranges. The glutamate-binding domains from ionotropic glutamate receptors dimerize and plausibly offer a starting scaffold for engineering an indicator that binds two glutamates per molecule. Alternatively, iGluSnFR molecules could be daisy-chained, likely with exogenous dimerization domains, to produce cooperative indicators. This research aim is quite speculative—it would likely take a great deal of effort to produce useful sensors, but the payoff may be worth it.

10 Conclusion and Outlook

Glutamate serves as the principal excitatory neurotransmitter in all vertebrates and many invertebrates. It also subserves many other roles, including occasional inhibition and function at the neuromuscular junction in some organisms and critical functions in metabolism. Glutamatergic synapses are densely distributed throughout the vertebrate brain. Their density, estimated to be around ~1 synapse per cubic micrometer, underscores the prevalence and significance of glutamate signaling in neural circuits. The precise regulation of glutamate release, uptake, and clearance is essential for maintaining proper synaptic function and ensuring the balance between excitation and inhibition in the nervous system.

Methods for detecting glutamate are of utmost importance in unraveling the intricate functioning of synapses and neural circuits in various physiological contexts, ranging from normal physiology to development and disease. Direct visualization of glutamatergic signaling events has become relatively routine with glutamate-sensitive reporters. By using these reporters to study glutamate dynamics, researchers can gain insights into the mechanisms underlying synaptic plasticity, development, and the pathophysiology of various neurological disorders—among others. Accurately detecting and monitoring glutamate levels and fluctuations in different preparations and model organisms is critical for understanding the underlying mechanisms of these disorders and developing potential therapeutic interventions.

Here, we focus on the present state-of-the-art genetically encoded glutamate indicator, iGluSnFR3, which allows robust, reproductible in vivo detection of glutamate with single-vesicle sensitivity. We describe multiple aspects of iGluSnFR3, including sensor design and mechanism of action, in vivo imaging capabilities, detailed protocols for imaging iGluSnFR3, and future development of the indicator. We provide detailed protocols for using iGluSnFR3 in various preparations and animals, such as bacteria, tissue culture, brain slices, worms, larval and adult flies, fish, and rodents, to facilitate users to design and execute a host of experiments. Other imaging modalities and preparations (e.g., organoids) are possible, and iGluSnFR has even been used successfully in nonhuman primates [75] and plants [76]. It is likely that many outstanding questions about glutamatergic signaling will be answered in the coming decades using this indicator.

Further headroom likely remains in optimizing iGluSnFR function through protein engineering. High priority should be placed on the improvement of variants in colors other than green, particularly red or far-red, which would facilitate two-color and deep imaging.

References

1. Hayashi T (1954) Effects of sodium glutamate on the nervous system. Keio J Med 3:183–192
2. Watkins JC (2000) l -Glutamate as a central neurotransmitter: looking back. Biochem Soc T 28:297–310
3. Watkins JC, Jane DE (2006) The glutamate story. Br J Pharmacol 147:S100–S108
4. Curtis DR, Phillis JW, Watkins JC (1961) Actions of amino-acids on the isolated hemisected spinal cord of the toad. Br J Pharm Chemoth 16:262–283
5. Biscoe TJ et al (1977) D-α-Aminoadipate as a selective antagonist of amino acid-induced and synaptic excitation of mammalian spinal neurones. Nature 270:743–745
6. Diamond JS, Jahr CE (1997) Transporters buffer synaptically released glutamate on a submillisecond time scale. J Neurosci 17:4672–4687
7. Diamond JS (2002) A broad view of glutamate spillover. Nat Neurosci 5:291–292
8. Stuart GJ, Spruston N (2015) Dendritic integration: 60 years of progress. Nat Neurosci 18:1713–1721
9. Nicholls DG, Sihra TS (1986) Synaptosomes possess an exocytotic pool of glutamate. Nature 321:772–773
10. Lorimier RMD et al (2002) Construction of a fluorescent biosensor family. Protein Sci 11:2655–2675
11. Okumoto S et al (2005) Detection of glutamate release from neurons by genetically encoded surface-displayed FRET nanosensors. Proc Natl Acad Sci 102:8740–8745
12. Tsien RY (2005) Building and breeding molecules to spy on cells and tumors. FEBS Lett 579:927–932
13. Hires SA, Zhu Y, Tsien RY (2008) Optical measurement of synaptic glutamate spillover and reuptake by linker optimized glutamate-sensitive fluorescent reporters. Proc Natl Acad Sci 105:4411–4416
14. Zhang Y et al (2023) Fast and sensitive GCaMP calcium indicators for imaging neural populations. Nature 615:884–891
15. Tian L et al (2009) Imaging neural activity in worms, flies and mice with improved GCaMP calcium indicators. Nat Methods 6:875–881
16. Marvin JS et al (2013) An optimized fluorescent probe for visualizing glutamate neurotransmission. Nat Methods 10:162–170
17. Franke K et al (2017) Inhibition decorrelates visual feature representations in the inner retina. Nature 542:439–444
18. Marvin JS et al (2018) Stability, affinity, and chromatic variants of the glutamate sensor iGluSnFR. Nat Methods 15:936–939
19. Pédelacq J-D, Cabantous S, Tran T, Terwilliger TC, Waldo GS (2006) Engineering and

characterization of a superfolder green fluorescent protein. Nat Biotechnol 24:79–88

20. Liu R, Li Z, Marvin JS, Kleinfeld D (2019) Direct wavefront sensing enables functional imaging of infragranular axons and spines. Nat Methods 16:615–618
21. Kazemipour A et al (2019) Kilohertz frame-rate two-photon tomography. Nat Methods 16:778–786
22. Aggarwal A et al (2023) Glutamate indicators with improved activation kinetics and localization for imaging synaptic transmission. Nat Methods 20:925–934
23. Lai S-L, Lee T (2006) Genetic mosaic with dual binary transcriptional systems in *Drosophila*. Nat Neurosci 9:703–709
24. Brand AH, Perrimon N (1993) Targeted gene expression as a means of altering cell fates and generating dominant phenotypes. Development 118:401–415
25. del Rodríguez AV, Didiano D, Desplan C (2012) Power tools for gene expression and clonal analysis in *Drosophila*. Nat Methods 9: 47–55
26. Phan TV et al (2024). Direct measurement of dynamic attractant gradients reveals breakdown of the Patlak–Keller–Segel chemotaxis model. PNAS. https://doi.org/10.1073/pnas.2309251121
27. Evans T (2006) Transformation and microinjection. In: Wormbook. https://doi.org/10.1895/wormbook.1.108.1
28. Rieckher M, Tavernarakis N (2017) P-body and stress granule quantification in *Caenorhabditis elegans*. Bio-Protocol 7:e2108
29. Frøkjær-Jensen C et al (2014) Random and targeted transgene insertion in *Caenorhabditis elegans* using a modified Mos1 transposon. Nat Methods 11:529–534
30. Frøkjær-Jensen C, Davis MW, Ailion M, Jorgensen EM (2012) Improved *Mos1*-mediated transgenesis in *C. elegans*. Nat Methods 9:117–118
31. Frøkjær-Jensen C et al (2008) Single-copy insertion of transgenes in *Caenorhabditis elegans*. Nat Genet 40:1375–1383
32. San-Miguel A, Lu H (2013) Microfluidics as a tool for *C. elegans* research. In: Wormbook, p 1–19. https://doi.org/10.1895/wormbook.1.162.1
33. Chronis N, Zimmer M, Bargmann CI (2007) Microfluidics for *in vivo* imaging of neuronal and behavioral activity in *Caenorhabditis elegans*. Nat Methods 4:727–731
34. Krajniak J, Lu H (2010) Long-term high-resolution imaging and culture of *C. elegans* in chip-gel hybrid microfluidic device for developmental studies. Lab Chip 10:1862–1868
35. McCormick KE, Gaertner BE, Sottile M, Phillips PC, Lockery SR (2011) Microfluidic devices for analysis of spatial orientation behaviors in semi-restrained *Caenorhabditis elegans*. PLoS One 6:e25710
36. Lewis JA, Fleming JT, McLafferty S, Murphy H, Wu C (1987) The levamisole receptor, a cholinergic receptor of the nematode *Caenorhabditis elegans*. Mol Pharmacol 31:185–193
37. Levamisole (0.25 mM). Cold Spring Harb Protoc 2009, pdb.rec11799 (2009)
38. Lycke R, Parashar A, Pandey S (2013) Microfluidics-enabled method to identify modes of *Caenorhabditis elegans* paralysis in four anthelmintics. Biomicrofluidics 7:064103
39. Katz M et al (2019) Glutamate spillover in *C. elegans* triggers repetitive behavior through presynaptic activation of MGL-2/mGluR5. Nat Commun 10:1882
40. Ashida K, Shidara H, Hotta K, Oka K (2020) Optical dissection of synaptic plasticity for early adaptation in *Caenorhabditis elegans*. Neuroscience 428:112–121
41. Wang Y et al (2020) Flexible motor sequence generation during stereotyped escape responses. elife 9:e56942
42. Kakanj P, Eming SA, Partridge L, Leptin M (2020) Long-term *in vivo* imaging of *Drosophila* larvae. Nat Protoc 15:1158–1187
43. Stork T, Sheehan A, Tasdemir-Yilmaz OE, Freeman MR (2014) Neuron-Glia interactions through the heartless FGF receptor signaling pathway mediate morphogenesis of *Drosophila* astrocytes. Neuron 83:388–403
44. Yu Y et al (2020) PICALM rescues glutamatergic neurotransmission, behavioural function, and survival in a *Drosophila* model of Aβ42 toxicity. Hum Mol Genet 29:ddaa125
45. Zabihihesari A, Hilliker AJ, Rezai P (2019) Fly-on-a-Chip: microfluidics for *Drosophila melanogaster* studies. Integr Biol 11:425–443
46. Badre NH, Martin ME, Cooper RL (2005) The physiological and behavioral effects of carbon dioxide on *Drosophila melanogaster* larvae. Comp Biochem Physiol Part Mol Integr Physiol 140:363–376
47. Sandstrom DJ (2008) Isoflurane reduces excitability of *Drosophila* Larval Motoneurons by activating a hyperpolarizing leak conductance. Anesthesiology 108:434–446
48. Cevik D et al (2019) Chloroform and desflurane immobilization with recovery of viable *Drosophila* larvae for confocal imaging. J Insect Physiol 117:103900

49. Pavel MA, Petersen EN, Wang H, Lerner RA, Hansen SB (2020) Studies on the mechanism of general anesthesia. Proc Natl Acad Sci 117: 13757–13766
50. Ji H, Han C, Larva SPA (2020) A method for mounting *Drosophila* Larva for long-term time-lapse imaging. J Vis Exp. https://doi.org/10.3791/60792
51. Richter FG, Fendl S, Haag J, Drews MS, Borst A (2018) Glutamate Signaling in the Fly visual system. Iscience 7:85–95
52. Molina-Obando S et al (2019) ON selectivity in the *Drosophila* visual system is a multisynaptic process involving both glutamatergic and GABAergic inhibition. elife 8:e49373
53. Lemon WC et al (2015) Whole-central nervous system functional imaging in larval *Drosophila*. Nat Commun 6:7924
54. Simpson JH, Looger LL (2018) Functional imaging and Optogenetics in *Drosophila*. Genetics 208:1291–1309
55. Akin O, Bajar BT, Keles MF, Frye MA, Zipursky SL (2019) Cell-type-specific patterned stimulus-independent neuronal activity in the *Drosophila* visual system during synapse formation. Neuron 101:894–904.e5
56. Matulis CA, Chen J, Gonzalez-Suarez AD, Behnia R, Clark DA (2020) Heterogeneous temporal contrast adaptation in *Drosophila* direction-selective circuits. Curr Biol 30:222–236.e6
57. MacDonald RB, Kashikar ND, Lagnado L, Harris WA (2017) A novel tool to measure extracellular glutamate in the zebrafish nervous system *in vivo*. Zebrafish 14:284–286
58. Kwan KM et al (2007) The Tol2kit: a multisite gateway-based construction kit for Tol2 transposon transgenesis constructs. Dev Dyn 236: 3088–3099
59. Stewart AM, Braubach O, Spitsbergen J, Gerlai R, Kalueff AV (2014) Zebrafish models for translational neuroscience research: from tank to bedside. Trends Neurosci 37:264–278
60. Antinucci P, Hindges R (2016) A crystal-clear zebrafish for *in vivo* imaging. Sci Rep-uk 6: 29490
61. Faveri FD, Marcotti W, Ceriani F (2021) Sensory adaptation at ribbon synapses in the zebrafish lateral line. J Physiol 599:3677–3696
62. Turan F et al (2021) Effect of modulating glutamate signaling on myelinating oligodendrocytes and their development—a study in the zebrafish model. J Neurosci Res 99:2774–2792
63. Collymore C, Tolwani A, Lieggi C, Rasmussen S (2014) Efficacy and safety of 5 anesthetics in adult zebrafish (Danio rerio). J Am Assoc Lab Anim Sci Jaalas 53:198–203
64. Trapani JG, Nicolson T (2010) Chapter 8: physiological recordings from zebrafish lateral-line hair cells and afferent neurons. Methods Cell Biol 100:219–231
65. Afrashteh N et al (2021) Spatiotemporal structure of sensory-evoked and spontaneous activity revealed by mesoscale imaging in anesthetized and awake mice. Cell Rep 37: 110081
66. Nazari M et al (2023) Regional variation in cholinergic terminal activity determines the non-uniform occurrence of cortical slow waves during REM sleep in mice. Cell Rep 42:112450
67. Hefendehl JK et al (2016) Mapping synaptic glutamate transporter dysfunction *in vivo* to regions surrounding Aβ plaques by iGluSnFR two-photon imaging. Nat Commun 7:13441
68. Xie Y et al (2016) Resolution of high-frequency mesoscale intracortical maps using the genetically encoded glutamate sensor iGluSnFR. J Neurosci 36:1261–1272
69. Madisen L et al (2015) Transgenic mice for intersectional targeting of neural sensors and effectors with high specificity and performance. Neuron 85:942–958
70. Helmchen F, Denk W (2005) Deep tissue two-photon microscopy. Nat Methods 2:932–940
71. Dana H et al (2016) Sensitive red protein calcium indicators for imaging neural activity. elife 5:e12727
72. Podgorski K, Ranganathan G (2016) Brain heating induced by near-infrared lasers during multiphoton microscopy. J Neurophysiol 116: 1012–1023
73. Wu J et al (2018) Genetically encoded glutamate indicators with altered color and topology. ACS Chem Biol 13:1832–1837
74. Hirano M et al (2022) A highly photostable and bright green fluorescent protein. Nat Biotechnol 40:1132–1142
75. Macknik SL et al (2019) Advanced circuit and cellular imaging methods in nonhuman primates. J Neurosci 39:8267–8274
76. Toyota M et al (2018) Glutamate triggers long-distance, calcium-based plant defense signaling. Science 361:1112–1115